Visual Simulation of Weathering By γ-ton Tracing

Yanyun Chen Lin Xia* Tien-Tsin Wong† Xin Tong Hujun Bao* Baining Guo Heung-Yeung Shum

Microsoft Research Asia *Zhejiang University †The Chinese University of Hong Kong

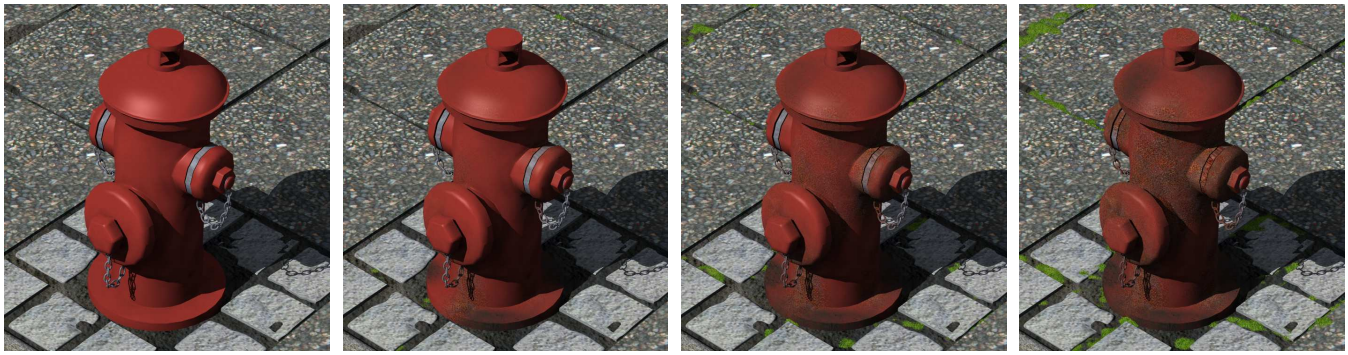

Figure 1: A weathering sequence generated by our system. From left to right, the hydrant becomes increasingly rusty and dusty. The gap between the tiles becomes colonized by moss.

Abstract

Weathering modeling introduces blemishes such as dirt, rust, cracks and scratches to virtual scenery. In this paper we present a visual simulation technique that works well for a wide variety of weathering phenomena. Our technique, called γ-ton tracing, is based on a type of aging-inducing particles called γ-tons. Modeling a weathering effect with γ-ton tracing involves tracing a large number of γ-tons through the scene in a way similar to photon tracing and then generating the weathering effect using the recorded γ-ton transport information. With this technique, we can produce weathering effects that are customized to the scene geometry and tailored to the weathering sources. Several effects that are challenging for existing techniques can be readily captured by γ-ton tracing. These include global transport effects, or "stain-bleeding". γ-ton tracing also enables visual simulations of complex multi-weathering effects. Lastly γ-ton tracing can generate weathering effects that not only involve texture changes but also large-scale geometry changes. We demonstrate our technique with a variety of examples.

Keywords: Rendering, appearance modeling, texturing, material models

1 Introduction

Weathering modeling introduces blemishes such as dirt, rust, cracks and scratches to virtual scenery. It is an important cue in photo-realism as weathering effects appear everywhere in our daily life. Traditionally, blemishes are generated by combining many hand-painted textures. This process is labor intensive, especially if a weathering sequence has to be painted by hand and the consistency between consecutive frames is maintained manually. Physically-based techniques [Dorsey and Hanrahan 2000] can automatically simulate a number of aging effects. A drawback of this approach, however, is that a new model has to be developed for each specific effect with detailed understanding of the underlying physical process. In addition, sometimes a physically-based simulation is not possible because the aging process (physical, chemical, biological, and combinations thereof) is not fully understood or too complex to simulate.

In this paper we present a visual simulation technique that works well for a wide variety of weathering phenomena. Our technique, called *γ-ton tracing*, is based on a type of aging-inducing particles called γ-tons (pronounced as "gamma-ton"). γ-ton is named after the Greek word "$\gamma\epsilon\rho os$" or "$\gamma\eta\rho\alpha\iota os$", which means "old". Generating a weathering effect with γ-ton tracing is an iterative process. Each iteration generates a frame of a weathering sequence through two passes. In the first pass, γ-tons are emitted from γ-ton sources and are traced through the scene in a way similar to photon tracing [Jensen 1996]. The result of the first pass is a *γ-ton map* describing the γ-ton transport information within the scene. From the γ-ton map, the second pass generates the actual weathering effect by modifying surface material properties and geometry through multi-texturing, texture synthesis, or displacement mapping. Through γ-ton tracing iterations, the cumulative weathering effect over time can be modeled. Fig. 1 shows a weathering sequence generated by our system. Note that the hollow gaps between tiles tend to collect more "humidity" brought by γ-tons from the protrusive tile surface and thus are easily colonized by the moss. Once the areas being colonized, they tend to trap more humidity and hence result in spotty growth of moss.

The *γ-ton sources* model the sources of aging, which come in the forms of point, area, or environment sources. A point source is appropriate for effects such as a dribble of rust down a wall from a leaky pipe, whereas an environment source is suitable for aging effects caused by ambient factors such as air pollution. γ-tons emitted from γ-ton sources propagate through the scene, interacting with surfaces. At each surface point, a surface property called *γ-reflectance* is defined that affects the paths through which incident γ-tons are deflected. For efficiency, the actual paths of γ-tons are determined probabilistically by the γ-reflectance of interacting surfaces using Russian roulette. The interaction of γ-tons with surfaces not only affects the γ-ton paths, but also enables *γ-transport*. Specifically, a γ-ton impinging at a surface point can pick up blemishes from that point and deposit them in subsequent

*This work was done while Lin Xia was a visiting student at Microsoft Research Asia.

surface interactions.

With γ-ton tracing, we can generate aging effects that are customized to scene geometry and tailored to aging sources [Miller 1994; Wong et al. 1997]. Through iterative γ-ton tracing, an aging sequence can be easily produced with consistency between consecutive frames. The iterative nature of γ-ton tracing also allows us to modify the γ-reflectance of surfaces using the γ-ton map from the previous iteration and thus affect the γ-ton tracing in subsequent iterations. This is useful for modeling a variety of aging effects, e.g., the real-world phenomenon of already rusty areas rusting faster can be modeled via iterative updating the γ-reflectance of the rusty area so as to trap more rust-inducing γ-tons.

γ-transport is an important feature of γ-ton tracing. With this feature we can readily capture *global transport* effects, or "stain-bleeding." Furthermore, because blemishes of one area can be transported to another area undergoing a different type of aging process, γ-transport enables visual simulations of complex *multi-weathering* effects that result from multiple co-existing and interacting weathering processes. Simulation of the global transport effects is difficult with existing techniques. Multi-weathering effects are possible with physically-based simulations in principle. However, simultaneously running multiple physically-based simulations and managing their interactions is a daunting task, and we are not aware of any such attempts in weathering simulation.

Another important feature of γ-ton tracing is that it can generate weathering effects that not only involve texture changes but also geometry changes. Large-scale geometry changes are achieved by working through iterations. The geometry change in each iteration is implemented as a displacement map defined according to the γ-ton map. In the next iteration, the γ-ton tracing and displacement mapping are performed on top of the displaced geometry from the previous iteration. For this reason, large-scale geometry changes such as those in corrosive and erosive weathering can be achieved with our technique. Large-scale geometry changes are challenging for existing techniques. For example, in [Dorsey et al. 1999; Cutler et al. 2002] geometry changes are constrained to take place within a set of slabs or layers aligned with the aging surfaces.

2 Related Work

Procedural texturing [Cook 1984; Ebert et al. 1998] is a traditional approach for creating irregular patterns and shapes. Perlin noise [Perlin 1985] is a widely-used for modeling stochastic textures. Turk [1991] and Witkin and Kass [1991] introduced reaction-diffusion textures inspired by biochemical processes. Gobron and Chiba [2001] simulated the crack patterns using 3D surface cellular automata.

Badler and Becket [1990] modeled blemishes based on fractal subdivision techniques and relatively simple distribution models. Miller [1994] and Hsu and Wong [1995] found out that the distribution of blemishes is strongly geometry-dependent and related it to the accessibility and exposure maps respectively. Early approaches, including accessibility and exposure maps, do not actually go through a weathering simulation process over time. In fact, they directly model the final appearance and use the strength of the weathering effect (accessibility or exposure) to mimic the growth of weathering. Therefore, significant manual intervention is needed in order to convincingly match natural phenomena.

Physically-based simulation fully automates the simulation of weathering and obtains realistic results. Dorsey et al. [1996] simulated surface appearance changes as the result of rainwater flowing over surfaces over a long period of time. Paquette et al. [2002] captured paint cracks and peelings. Merillou et al. [2001] examined metal corrosion. Bosch et al. [2004] studied scratches. Desbenoit et al. [2004] modeled lichen growth. Sometimes the simulations need to reach subsurface level to faithfully portray certain weathering effects. This is the case with metallic patina [Dorsey and Hanrahan 1996] as well as stone weathering [Dorsey et al. 1999]. In contrast to the physically-based approach, the visual simulation approach which we follow aims to achieve desirable visual effects rather than physically accurate simulation processes.

Many weathering effects involve both texture and geometry changes. For terrains (height fields), geometry changes as a result of erosion are examined in [Kelley et al. 1988; Musgrave et al. 1989]. For (non-height-field) objects, small-scale geometry changes are demonstrated in [Dorsey et al. 1999], [Gobron and Chiba 2001] and [Paquette et al. 2001]. Cutler et al. [2002] employed physically-based weathering simulations as geometric authoring tools to construct layer-based representation of solid objects. In their systems, effects of different weathering simulations are applied separately to different layers. Complex interactions between these effects are ignored.

3 The γ-ton Tracing

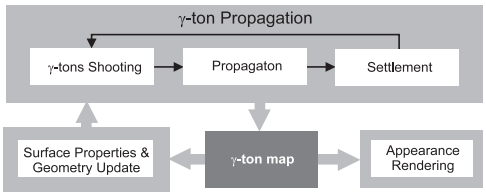

Figure 2: The overview of γ-ton tracing.

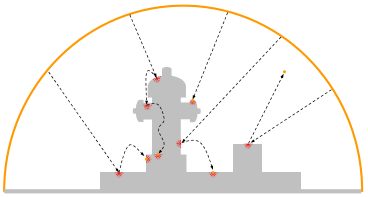

Figure 3: γ-tons shot from the hemispherical environment γ-ton source bounce in the scene and induce weathering.

The proposed framework is summarized in Fig. 2. The core is the iterative γ-ton propagation. It resembles classical photon tracing [Jensen 1996]. Within each iteration, thousands of γ-tons are created and shot from the γ-*ton source*. As γ-tons propagate in the scene, they catalyse weathering on any encountered surfaces (Fig. 3). Their propagation is *stochastically* determined by their *motion probabilities* and the γ-*reflectance* of the encountered surfaces. At each encounter, they may pick up or deposit substances on the surface. Such transport of substances determines the distribution of blemishes.

To precisely record the stochastic weathering contribution by γ-tons and to represent the local surface attributes, we generate a point-based model [Pfister et al. 2000; Rusinkiewicz and Levoy 2000] from the input scene by resampling (Fig. 4). Each generated surfel maintains its own γ-reflectance and material properties. While γ-reflectance affects how the incident γ-tons deflect, material properties keep track of the essential substances for weathering. The blemish being modeled is one of these material properties. The accumulation of blemish over all surfels forms the distribution of blemishes, the γ-*ton map*. This point-based γ-ton map allows us to handle a wide range of geometric representations of input scenery.

The weathering induced by γ-tons changes the surface properties which in turn affects the subsequent iterations of γ-propagation. For example, once the surface is rusty, its roughness increases and helps to trap more γ-tons. The result is an increase in rusting rate. We update the surface properties based on the γ-ton map obtained from the last iteration. In cases such as corrosion and erosion, we also displace the geometry according to the γ-ton map. Large-scale and cumulative erosive weathering is achieved through iterative tracing of γ-tons on deformed geometry. With the γ-ton map,

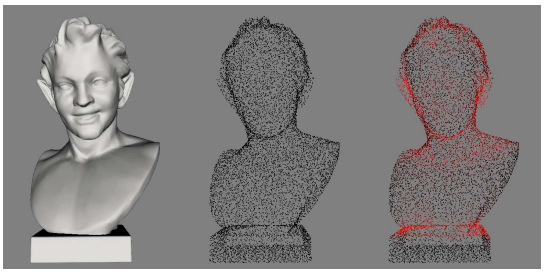

Figure 4: The original model (left) is resampled into a point-based representation (middle). After γ-ton tracing, we obtain the γ-ton map over surfels (right) indicating the value distribution of blemishes. Here the γ-ton map (shown in red) indicates the presence of metallic patina.

the stochastic visual appearance of weathering can be rendered with different levels of texturing and procedural techniques, including multi-texturing, displacement mapping, and texture synthesis. The choice depends on the nature of weathering. The growth of weathering can be rendered with frame consistency according to the time-ordered sequence of γ-ton maps.

3.1 The γ-ton and γ-ton Sources

Each γ-ton bears two main kinds of attributes, motion and carrier. Motion probabilities account for its motion behavior while the carrier attributes account for the substances being carried. These motion probabilities are compulsory attributes for all γ-tons, but the carrier attributes are extensible depending on the weathering effect being modeled. The following shows the attributes of an example γ-ton:

```
Ton {
    Motion probabilities:
        k_s, k_p, k_f;  // Probability of propagating along a straight line,
                        // parabolic curve, or flowing
    Carrier attributes:
        s_h;            // Humidity
        s_d;            // Amount of dirt
        s_f;            // Amount of fungus
        ...
}
```

The path of a γ-ton is stochastically determined by its motion probabilities (k_s, k_p, k_f). At any time, a γ-ton can only be in one of the four basic motion states (Fig. 5): propagating in space along a straight line, propagating in space along a parabolic trajectory, adhering and flowing on a surface, or settling on a surface. Motion probabilities represent the motion energy of a γ-ton. A γ-ton propagates in the first three ways as long as it retains sufficient energy. Once it runs out of energy, it settles down. The path of a γ-ton is parabolic if it propagates in space and carries weight. The sum of all motion probabilities must be less than or equals to one, i.e., $k_s + k_p + k_f \leq 1$. Hence, the probability of settling is implicitly represented as $(1 - k_s - k_p - k_f)$. These motion probabilities do not change until the γ-ton impinges upon a surface, where these probabilities change according to the γ-reflectance of the surface (explained shortly).

The carrier attributes account for any possible substance being carried by γ-ton during transport. The number of attributes is scalable and depends on the weathering effect being modeled. In addition to weathering-catalysing γ-tons, one can also design weathering-resisting γ-tons which carry weathering-resistant substances. For example, γ-tons can carry "heat" substance to mimic the sunshine which reduces corrosive substances such as "humidity" on a metallic surface.

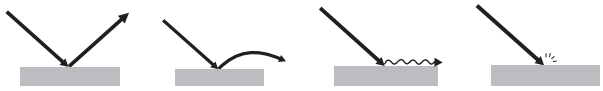

(a) reflect (b) bounce (c) flow (d) settled

Figure 5: Four possible motions of a γ-ton after impinging upon a surface.

To mimic the wide variety of natural aging sources, the γ-ton sources can be in the form of point, area, and environment sources. A point source, for example, can be used to model the dribble of rust from a leaky pipe. Fig. 10 shows the weathering effect modeled by a "spotlight" γ-ton source (a special case of point source). It shoots γ-tons within a restricted range of directions. Atmospheric weathering exhibits "ambient"-like effects that can be accounted for by environment sources. For most examples in this paper, we employed two γ-ton sources: an enclosing environment source (see Fig. 3) and an overhead area source which emits γ-tons vertically downward.

3.2 γ-reflectance and Material Property

Corresponding to the motion and carrier attributes of γ-tons, there are two kinds of surface properties, *γ-reflectance* and *material property*. γ-reflectance $(\Delta_s, \Delta_p, \Delta_f)$ determines how incident γ-tons deflect. Material properties record the amount of blemish or other substances on a surface. The following shows an example property list of a surfel.

```
Surf {
    γ-reflectance:
        Δ_s, Δ_p, Δ_f;  // Deterioration rate for k_s, k_p, & k_f
    Material properties:
        s_h;            // Humidity
        s_d;            // Amount of dirt
        s_f;            // Amount of fungus
        ...
}
```

While γ-reflectance is compulsory, material properties are extensible depending on the weathering being modeled. For instance, if the growth of moss is being modeled, the amount of moss seed can be introduced both as a carrier attribute of γ-ton and a material property of surfaces.

When a γ-ton impinges on a surface, its motion probabilities (k'_s, k'_p, k'_f) are deteriorated according to the following set of simple equations.

$$k'_s = \max(k_s - \Delta_s, 0) \quad (1)$$

$$k'_p = \max(k_p - \Delta_p, 0) \quad (2)$$

$$k'_f = \max(k_f + \max(k_p - \Delta_p, 0) - \Delta_f, 0) \quad (3)$$

Our rationale to fix the deterioration equations is to free the user from tuning an excessive number of parameters. The initial surface attribute values can be set by the user.

3.3 γ-ton Propagation and γ-transport

A γ-ton is emitted from a source along a straight line. The direction of travel is stochastically determined by the property of the γ-ton source as in photon tracing [Jensen 1996]. The γ-ton bounces in the scene until it settles down on a surface or flies out of the scene. Whenever a γ-ton impinges on a surface, Russian roulette [Spanier and Gelbard 1969; Arvo and Kirk 1990] is employed to determine its new motion probabilities. As in photon tracing, we use a uniformly distributed random variable $\xi \in [0, 1]$ and make the following decision: reflect if $\xi \in [0, k_s]$, bounce if $\xi \in (k_s, k_s + k_p]$, flow if $\xi \in (k_s + k_p, k_s + k_p + k_f]$, and settle otherwise. For reflected or bounced γ-tons, we regard the surface as "diffuse" and evenly distribute the outgoing directions over the upper hemisphere centered at the surface point. Unless the γ-ton settles on the surface, its motion probabilities are modified according to the local γ-reflectance of the surface and the γ-ton continues to travel with the new motion probabilities. For a bounced γ-ton, the distance of a bounce is

a parameter the user supplies for each type of γ-ton in our current system.

As a γ-ton propagates, it picks up and deposits substances on the interacting surfels. We call this behavior γ-transport (Fig. 6). It is this removal and introduction of substances that causes weathering.

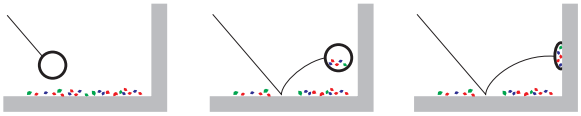

Figure 6: γ-transport by a γ-ton.

For simplicity, all γ-transports are defined in the following simple form: $a \leftarrow a + b \cdot k$, where a and b are either carrier attributes of the γ-ton or material properties of the interacting surface. k is a scalar weight. For instance, we can describe the dust contribution s_d of a dust-carrying γ-ton `Ton` to a surface `Surf` as follows: $\texttt{Surf}.s_d \leftarrow \texttt{Surf}.s_d + \texttt{Ton}.s_d \cdot k$. With a series of such simple γ-transports, complex weathering effects can be modeled as we shall see in Section 4. In this regard, a series of γ-transports resembles a surface shader [Cook 1984].

During γ-ton propagation, we trace the path of the γ-ton and find the surface being intersected. For a γ-ton traveling in a straight line, the intersection test is the same as that of ray tracing. For a γ-ton traveling along a parabolic curve, its trajectory is piecewise linearly approximated. For a γ-ton flowing on a surface, the γ-ton moves a small step along the tangent direction of the surface and interacts with the surface at the new position. The step size is a constant for a given type of γ-ton and is specified by the user.

We perform the intersection test on the original surface model and utilize a spatial partitioning scheme designed for ray-tracing to accelerate the test. Once the point of intersection is computed, we look up the nearby surfels. The look-up is accelerated by organizing all surfels in a kd-tree.

3.4 Surface Properties and Geometry Update

γ-ton propagation and γ-transport change the original surface properties. For instance, the introduction of rust particles increases the surface roughness, which in turn affects the γ-reflectance. We update these surface properties based on the γ-ton map obtained from the previous iteration. The user can define a simple function for this update. In cases such as corrosion and erosion, the geometry is also deformed according to the γ-ton map; we shall describe the relevant details in Section 4. The cumulative weathering effects are accomplished through performing such updates iteratively.

3.5 A Tutorial Example

We illustrate the system with the visual simulation of metallic patina. A spherical environment γ-ton source is used to shoot γ-tons with the following attribute values:

```
Ton {
        k_s = 1;   k_p = 0;   k_f = 0;
        s_p = 1;  // Amount of patina
}
```

which means the γ-tons travel in a straight line ($\texttt{Ton}.k_s = 1$) and carry patina ($\texttt{Ton}.s_p = 1$). The surface property of a copper surface is initialized as

```
Surf {
        Δ_s = 0.5;   Δ_p = 0;   Δ_f = 0;
        s_p = 0;  // Initially, no patina
}
```

It means the original surface is highly reflective and no patina is present initially. A settled γ-ton introduces patina to the surface according to the following γ-transport rule:

$$\texttt{Surf}.s_p \leftarrow \texttt{Surf}.s_p + 0.05 \cdot \texttt{Ton}.s_p;$$

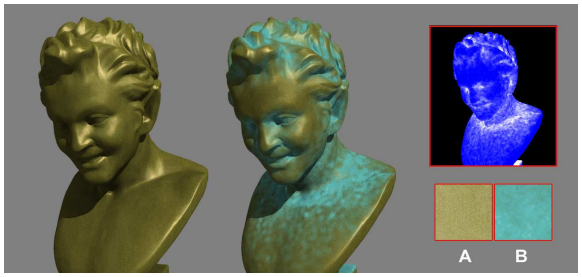

Figure 7: Patina on a bronze sculpture. The two textures used for appearance rendering are labeled as "A" and "B".

Since the motion probability k_s of a γ-ton `Ton` drops significantly with each bounce, about half number of γ-tons will settle down after first bounce and the remains bounce twice. As a result, a region with low accessibility can easily trap motion-deteriorated γ-tons and accumulate patina. Fig. 7 shows the result (middle) and the underlying γ-ton map (right).

The weathering appearance is rendered by multi-texturing with two textures, one with patina and one without (shown in Fig. 7). The γ-ton map values are used to blend these two textures by a simple alpha-blending. Most images in this paper are rendered using this method.

Through this example, we wish to demonstrate that γ-ton tracing can effectively generate convincing weathering effects with little user effort. We reiterate that our technique is intended for capturing the visual effects of weathering phenomena. For physically-based simulation of metallic patina, see [Dorsey and Hanrahan 1996].

4 Application Examples

In this section we demonstrate γ-ton tracing with more complex examples. The companion video provides demonstrations of frame-consistent weathering sequences and complex interactions of multiple weathering.

Stain-Bleeding: A surface near stained surfaces tends to get stained *indirectly* by dirty water splattered or flown from the nearby stained surfaces. For example, the rusty chains in Fig. 8 cause rust stains on the staircase beneath. We call this phenomenon "stain-bleeding" since it is analogous to the "color-bleeding" effect in global illumination. It is straightforward to simulate "stain-bleeding" with γ-ton tracing because of the γ-transport capability of γ-tons.

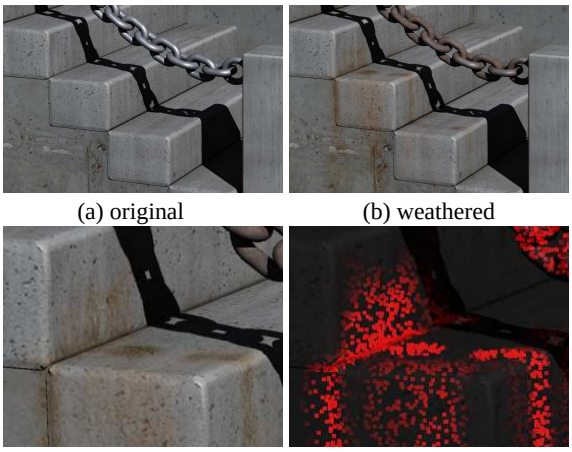

(a) original (b) weathered

(c) blow-up (d) γ-ton map

Figure 8: An example of "stain-bleeding".

The example in Fig. 8 is generated by γ-ton tracing followed by rendering through multi-texturing. The rendering method is the same as the one used for Fig. 7. Notice that γ-tons not only induce

rust on the iron chain, but also carry rust particles to the staircase. Two forms of "stain-bleeding" can be seen in this example, one due to bouncing and the other due to flowing. Notice the stain on the vertical face at the center of Fig. 8 (c). The bouncing γ-tons bring rust particles from the nearby stain spots on the steps to this vertical face. The flowing γ-tons further propagate stains downward, especially along the cracks. Notice the different stain patterns formed by bouncing and flowing γ-tons in the γ-ton map (Fig. 8 (d)).

For the example in Fig. 8, the motion probabilities of γ-tons are $(k_s, k_p, k_f) = (0.0, 0.8, 0.2)$, whereas γ-ton carrier attributes include humidity ($s_{humidity}$) and rust (s_{rust}) with initial values of $s_{humidity} = 1$ and $s_{rust} = 0$. For both the cement staircase and the metallic chain, γ-reflectance is $(\Delta_s, \Delta_p, \Delta_f) = (0.0, 0.4, 0.05)$ and material properties, including humidity and rust, are initialized as $s_{humidity} = 0$ and $s_{rust} = 0$. The γ-transport rules for the cement staircase and wall are

$$\begin{aligned} \texttt{Surf}.s_{humidity} &\leftarrow \texttt{Surf}.s_{humidity} + 0.1 \cdot \texttt{Ton}.s_{humidity}; \\ \texttt{Surf}.s_{rust} &\leftarrow \texttt{Surf}.s_{rust} + 0.1 \cdot \texttt{Ton}.s_{rust}; \end{aligned}$$

while the γ-transport rule for the metallic chain is

$$\texttt{Surf}.s_{humidity} \leftarrow \texttt{Surf}.s_{humidity} + 0.1 \cdot \texttt{Ton}.s_{humidity};$$

And the γ-transport rule for γ-tons is

$$\texttt{Ton}.s_{rust} \leftarrow \texttt{Ton}.s_{rust} + \texttt{Surf}.s_{rust};$$

This rule represents the transfer of rust particles from the chain to γ-tons. After each γ-ton tracing iteration, we update the surface properties of the chain as follows

$$\begin{aligned} \texttt{Surf}.s_{rust} &\leftarrow \texttt{Surf}.s_{rust} + 0.015 \cdot \texttt{Surf}.s_{humidity}; \\ \texttt{Surf}.s_{humidity} &\leftarrow \texttt{Surf}.s_{humidity} - 0.5 \cdot \texttt{Surf}.s_{humidity}; \end{aligned}$$

More examples of stain-bleeding can be found in Fig. 13.

Multi-Weathering: Several weathering effects often take place simultaneously and these weathering processes can interact with each other to generate more complex weathering effects. A distinct feature of our framework is that it can simulate multiple weathering processes and more importantly, their *interactions*. Such interactions cannot be simulated by individually modeling multiple weathering and blending their results. Our framework can simulate the complex interactions among multiple weathering processes because of the multiple γ-transport ability of γ-tons and the iterative updates of surface properties and geometry.

Fig. 9 shows our simulation of a multi-weathering scenario with two interacting weathering processes, moss growth on the ground and dirt splattering near the bottom of the cement wall. The ground is initialized with a large amount of dirt and a small number of seeds for the moss (Fig. 9 (a)). As γ-tons propagate through the scene, they can pick up materials (moss or dirt) from the ground and transport them to other places. If they pick up soil, they expedite "stain-bleeding" from the ground to the bottom of the cement wall. If they pick up moss, they facilitate the moss colonization. As the moss-covered areas grow, more soil is covered and thus less likely to be splattered onto the cement wall. In other words, the growth of moss suppresses the splattering of dirt onto the wall. We naturally model such interactions by modifying the γ-reflectance of the ground after each γ-ton tracing iteration. As a result, γ-tons become more likely to be trapped in moss-covered regions.

The result of multi-weathering can be seen by comparing Fig. 9 (b) and (c). The "stain-bleeding" (red γ-tons in Fig 9 (b)) is significantly suppressed by the growth of moss (blue γ-tons), especially on the left hand side of the scene. Such competition cannot be approximated by individually modeling two weathering effects (Fig. 9 (c) and (d)) and blending the results. The images are rendered by using multi-texturing the same way as for Fig. 7.

For Fig. 9, we use two types of γ-tons: $\texttt{Ton}(\texttt{rain})$ for the rain and $\texttt{Ton}(\texttt{moss})$ for moss seeds. The rain γ-ton motion probabilities

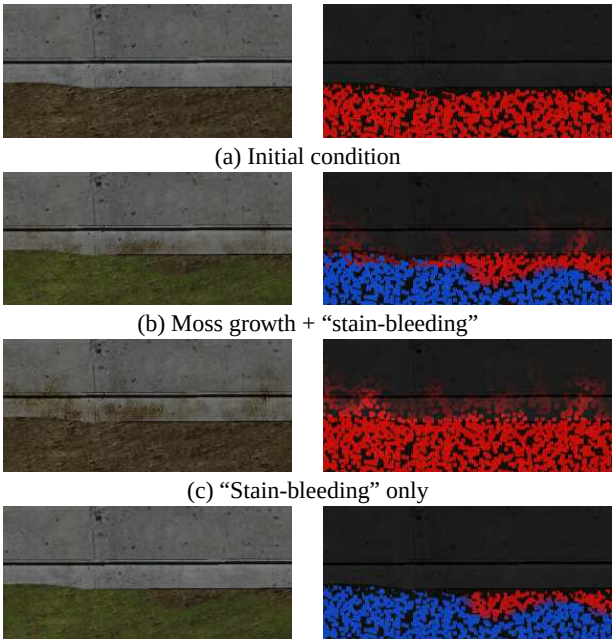

(a) Initial condition

(b) Moss growth + "stain-bleeding"

(c) "Stain-bleeding" only

(d) Moss growth only

Figure 9: An example of multi-weathering. The growth of moss suppresses the "stain-bleeding" from the ground to the cement wall. Left and right columns show the rendered images and the corresponding γ-ton maps respectively. The blue and red colors indicate the amount of moss and soil respectively.

are $(k_s, k_p, k_f) = (0.0, 0.8, 0.2)$, whereas the rain γ-ton carrier attributes are dirt $s_{dirt} = 0$ and moss $s_{moss} = 0$. The moss γ-ton motion probabilities are $(k_s, k_p, k_f) = (0.2, 0.0, 0.0)$, whereas the moss γ-ton carrier attributes are dirt $s_{dirt} = 0$ and moss $s_{moss} = 0$. For both the cement wall and the ground, their γ-reflectances are $(\Delta_s, \Delta_p, \Delta_f) = (0.0, 0.4, 0.05)$ and their material properties include dirt (s_{dirt}) and moss (s_{moss}). While the material properties of the cement wall are initialized as $s_{dirt} = 0$ and $s_{moss} = 0$, the material properties of the ground are initialized as $s_{dirt} = 1$ and $s_{moss} = 0$. The γ-transport rules for the ground are

$$\begin{aligned} \texttt{Surf}.s_{moss} &\leftarrow \texttt{Surf}.s_{moss} + \texttt{Ton}(\texttt{moss}).s_{moss}; \\ \texttt{Surf}.s_{moss} &\leftarrow \texttt{Surf}.s_{moss} + 0.02 \cdot \texttt{Ton}(\texttt{rain}).s_{moss}; \end{aligned}$$

The first rule is only used once at the beginning to initialize the ground with small number of moss seeds. The γ-transport rule for the cement wall is

$$\texttt{Surf}.s_{dirt} \leftarrow \texttt{Surf}.s_{dirt} + \texttt{Ton}(\texttt{rain}).s_{dirt};$$

And the γ-transport rules for the rain γ-ton are

$$\begin{aligned} \texttt{Ton}(\texttt{rain}).s_{moss} &\leftarrow \texttt{Ton}(\texttt{rain}).s_{moss} + 0.1 \cdot \texttt{Surf}.s_{moss}; \\ \texttt{Ton}(\texttt{rain}).s_{dirt} &\leftarrow \texttt{Ton}(\texttt{rain}).s_{dirt} + \texttt{Surf}.s_{dirt}; \end{aligned}$$

After each γ-ton tracing iteration we update the surface properties of the ground as follows

$$\texttt{Surf}.s_{dirt} \leftarrow \texttt{Surf}.s_{dirt} - 0.1 \cdot \texttt{Surf}.s_{moss};$$

More examples of multiple weathering are shown in Fig. 12. In our current implementation, we store the properties of all effects in a single layer (on surfels). It helps the users to easily specify the rules of the interaction between effects and ignore the complex underlying physics details. It also allows the user to simulate multiple effects on any surface and to render the effects with various methods. However, the single-layer representation also has limitations.

It is difficult to handle multiple weathering effects with some structural change of objects (e.g., dust accumulated in the cracks of an oil painting).

Geometry Changes: Fig. 11 shows an example of weathering that involves large-scale geometry change. This weathering sequence is generated by applying a displacement map to the Sphinx model after each γ-ton tracing iteration. The displacement map is determined by the γ-ton map, which is obtained by tracing a large number of γ-tons emitted from a hemispherical environment source. At each surface point, the incident γ-ton picks up materials from that point and deposits them at points of subsequent surface interactions. Consequently, some points in the γ-ton map gain a lot of mass while others loose mass. This information is used to obtain the displacement map. A mass-gaining point displaces along the positive direction of its surface normal and in an amount proportional to the mass gained. On the other hand, a mass-loosing point displaces similarly but along the negative direction of its surface normal. To facilitate the surface displacement, we retile the initial surface mesh using Turk's technique [Turk 1992]. This surface mesh is retiled after each application of displacement mapping to generate the deformed model for the next round of γ-ton tracing and displacement mapping.

Performance: The running time of γ-ton propagation depends on two major factors: the number of γ-tons emitted and the number of surfels. The scene in Fig. 12 is resampled into $100k$ surfels. Both Fig. 8 and 9 are snapshots of the scene shown in Fig. 12. Each γ-ton tracing iteration takes about 1 minute to trace the $15k$ γ-tons. For all examples in this paper, we run 30 iterations to generate the weathering sequence. The scene shown in Fig. 13 is also resampled into $100k$ surfels. Each iteration takes about $1.5 \sim 2$ minutes to trace $63k$ γ-tons. The scene shown in Fig. 1 is resampled into $50k$ surfels. Each iteration takes less than 1 minute to trace $7k$ γ-tons. Finally, the Sphinx model shown in Fig. 11 is resampled into $200k$ surfels. Each iteration takes about 3 minutes to trace $10k$ γ-tons and retile the mesh, which contains about $50k$ vertices. All these timings are measured on a PC with a 3 GHz Pentium IV processor.

5 Conclusions

We have presented a visual simulation framework that is effective for modeling a wide variety of weathering effects. With γ-ton tracing, the user can capture complex weathering phenomena with little effort. Some of these phenomena, such as "stain-bleeding", multi-weathering, and large-scale geometry changes have previously been challenging. A limitation of our current system is that it does not provide interactive visual feedbacks for choosing γ-ton tracing parameters since each γ-ton tracing iteration still takes a few minutes. A possible future work is to develop a preview technique similar to those used in the field of global illumination. In general, our work suggests that well-studied global illumination techniques have promising applications in the emerging field of appearance modeling and digital weathering [Dorsey and Hanrahan 2000]. We hope that our work inspires more interests in this promising direction.

Acknowledgement

The authors would like to thank Yaohua Hu for helpful discussions. Many thanks to Kyros Kutulakos for helping us coin the term γ-ton. Scenes in Fig. 1 and 11 are modeled by Mingdong Xie while the scene in Fig. 10 is modeled by Wei Zhou. We are grateful to the anonymous reviewers for their helpful suggestions and comments. Prof. Hujun Bao is supported in part by the 973 program of China (Grant No. 2002CB312102), National Natural Science Foundation of China (Grant No. 60021201) and Research Fund for Doctoral Program of Higher Education (Grant No.20030335083). Tien-Tsin Wong is supported in part by the Research Grants Council of the Hong Kong Special Administrative Region, under RGC Earmarked Grants (Project No. CUHK 4189/03E).

References

ARVO, J., AND KIRK, D. B. 1990. Particle transport and image synthesis. In *Proceedings of SIGGRAPH'90*, 63–66.

BADLER, N. I., AND BECKET, W. 1990. Imperfection for realistic image synthesis. *Journal of Visualization and Computer Animation 1*, 1 (Aug.), 26–32.

BOSCH, C., PUEYO, X., MERILLOU, S., AND GHAZANFARPOUR, D. 2004. A physically-based model for rendering realistic scratches. In *Proc. Eurographics 2004*.

COOK, R. L. 1984. Shade trees. In *Proceedings of SIGGRAPH '84*, 223–231.

CUTLER, B., DORSEY, J., MCMILLAN, L., MÜLLER, M., AND JAGNOW, R. 2002. A procedural approach to authoring solid models. *ACM Transactions on Graphics 21*, 3 (July), 302–311.

DESBENOIT, B., GALIN, E., AND AKKOUCHE, S. 2004. Simulating and modeling lichen growth. *Computer Graphics Forum 23*, 3, 341–350.

DORSEY, J., AND HANRAHAN, P. 1996. Modeling and rendering of metallic patinas. In *Proceedings of SIGGRAPH '96*, 387–396.

DORSEY, J., AND HANRAHAN, P. 2000. Digital materials and virtual weathering. *Scientific American* (February), 64–71.

DORSEY, J., PEDERSEN, H. K., AND HANRAHAN, P. 1996. Flow and changes in appearance. In *Proceedings of SIGGRAPH '96*, 411–420.

DORSEY, J., EDELMAN, A., JENSEN, H. W., LEGAKIS, J., AND PEDERSEN, H. K. 1999. Modeling and rendering of weathered stone. In *Proceedings of SIGGRAPH '99*, 225–234.

EBERT, D. S., MUSGRAVE, F. K., PEACHEY, D., PERLIN, K., AND WORLEY, S. 1998. *Texturing & Modeling: A Procedural Approach*, second ed. AP Professional.

GOBRON, S., AND CHIBA, N. 2001. Crack pattern simulation based on 3D surface cellular automata. In *The Visual Computer*, vol. 17(5). Springer, 287–309.

HSU, S.-C., AND WONG, T.-T. 1995. Simulating dust accumulation. *IEEE Computer Graphics & Applications 15*, 1, 18–22.

JENSEN, H. W. 1996. Global illumination using photon maps. In *Eurographics Rendering Workshop 1996*, 21–30.

KAJIYA, J. T. 1986. The rendering equation. In *Proceedings of SIGGRAPH '86*, 143–150.

KELLEY, A. D., MALIN, M. C., AND NIELSON, G. M. 1988. Terrain simulation using a model of stream erosion. In *Proceedings of SIGGRAPH '88*, 263–268.

MERILLOU, S., DISCHLER, J.-M., AND GHAZANFARPOUR, D. 2001. Corrosion: Simulating and rendering. In *Graphics Interface 2001*, 167–174.

MILLER, G. 1994. Efficient algorithms for local and global accessibility shading. In *Proceedings of SIGGRAPH '94*, ACM Press, 319–326.

MUSGRAVE, F. K., KOLB, C. E., AND MACE, R. S. 1989. The synthesis and rendering of eroded fractal terrains. In *Proceedings of SIGGRAPH '89*, 41–50.

PAQUETTE, E., POULIN, P., AND DRETTAKIS, G. 2001. Surface aging by impacts. In *Proceedings of Graphics Interface 2001*, 175–182.

PAQUETTE, E., POULIN, P., AND DRETTAKIS, G. 2002. The simulation of paint cracking and peeling. In *Proceedings of Graphics Interface 2002*, 59–68.

PERLIN, K. 1985. An image synthesizer. In *Proceedings of SIGGRAPH '85*, 287–296.

PFISTER, H., ZWICKER, M., VAN BAAR, J., AND GROSS, M. 2000. Surfels: surface elements as rendering primitives. In *Proceedings of SIGGRAPH '00*, 335–342.

RUSINKIEWICZ, S., AND LEVOY, M. 2000. Qsplat: a multiresolution point rendering system for large meshes. In *Proceedings of SIGGRAPH '00*, 343–352.

SPANIER, J., AND GELBARD, E. 1969. *Monte Carlo Principles and Neutron Transport Problems*. Addison-Wesley.

TURK, G. 1991. Generating textures for arbitrary surfaces using reaction-diffusion. *Computer Graphics (Proceedings of SIGGRAPH 91) 25*, 4 (July), 289–298.

TURK, G. 1992. Re-tiling polygonal surfaces. In *Computer Graphics (Proceedings of SIGGRAPH 92)*, vol. 26, 55–64.

WITKIN, A., AND KASS, M. 1991. Reaction-diffusion textures. *Computer Graphics (Proceedings of SIGGRAPH 91) 25*, 4 (July), 299–308.

WONG, T.-T., NG, W.-Y., AND HENG, P.-A. 1997. A geometry dependent texture generation framework for simulating surface imperfections. In *Proceedings of the 8-th Eurographics Workshop on Rendering (Rendering Techniques'97)*, 139–150.

Figure 10: The stain caused by dripping water. This weathering effect is simulated with a point γ-ton source.

Figure 11: Erosion of Sphinx after thousands of years.

Figure 12: A scene with “stain-bleeding” and multi-weathering effects.

Figure 13: Another scene with “stain-bleeding” effects (in the zoomed areas).